Journal of Materials Processing Technology 216 (2015) 339–347

Contents lists available at ScienceDirect

Journal of Materials Processing Technology

journal homepage: www.elsevier.com/locate/jmatprotec

Surface lubrication influence on electrode degradation during resistance spot welding of hot dip galvanized steel sheets

M. Spitz[a,*], M. Fleischanderl[b], R. Sierlinger[b], M. Reischauer[b], F. Perndorfer[b], G. Fafilek[c]

[a] CEST Kompetenzzentrum fuer elektrochemische Oberflaechentechnologie GmbH, Viktor Kaplan Strasse 2, 2700 Wiener Neustadt, Austria
[b] voestalpine Stahl GmbH, TKE, Forschung und Entwicklung, voestalpine-Strasse 3, 4020 Linz, Austria
[c] Institute of Chemical Technologies and Analytics, University of Technology Vienna, Getreidemarkt 9, 1060 Wien, Austria

ARTICLE INFO

Article history:
Received 18 September 2013
Received in revised form 8 September 2014
Accepted 10 September 2014
Available online 21 September 2014

Keywords:
Resistance spot welding
Surface lubrication
Hot dip galvanized steel sheet
Electrode degradation
Welding electrode
Wear

ABSTRACT

The material uptake mechanism of a resistance spot welding electrode is presented for two selected surface conditions of hot-dip galvanized steel sheets, i.e., lubricated and non-lubricated. The evolution of material deposition varies according to the different surface states. Spot welding of lubricated sheet results in a more uniform and reduced alloyed material uptake that deposits on the welding electrode cap. Accordingly, the low deposition of material on the electrode surface enhances the weldability of hot-dip galvanized steel sheets. A reproducible current flow and a stable energy input is thus ensured along the electrode cap surface during resistance spot welding. Furthermore, lubrication leads to a considerably reduced sticking of welding electrodes.

1. Introduction

Joining hot-dip galvanized steel sheets by means of resistance spot welding is today's industrial standard. Especially when manufacturing automobile assemblies, resistance spot welding is still, aside from laser welding and adhesive bonding, the leading joining process. Surface lubrication is a common method to protect steel sheet from corrosion during transportation. With consideration to the increasing demand for metallically coated steel sheet surfaces, not only corrosion protection but also stability during further processing is highly important. Specific surface-lubrication systems support the forming processes prior to the joining of all components. Improved resistance spot welding process stability is noticed by most users in the case of lubricated hot-dip galvanized steel sheets as opposed to non-lubricated ones. Lubrication mainly improves welding electrode life but also reduces sticking of the electrode on the surface. However, differences can be observed among different lubricants. To our knowledge, there is no detailed information concerning the influence of lubrication on the resistance of spot welding of hot-dip galvanized steel sheets. A discussion on the influence of lubrication on resistance spot welding of aluminum alloys can be found in Han et al. (2010) for different wax systems, and in Rashid et al. (2007) for lubrication-induced oxidation minimization. Both works aim at determining electrode life and not on the determination of an electrode degradation mechanism explicitly. Distinct benefits of different specific surface lubrications were observed in both works.

Diffusion of elements from steel sheet surfaces changes the welding electrode cap surface with respect to electrical and mechanical properties. It is known that zinc substantially influences welding electrode performance. Parker et al. (1998) showed that zinc diffusion leads to a pronounced transformation of the electrode surface composition, i.e., to an evolution of different brass alloys of varying zinc concentrations. This change in material property of different zones of varying alloy composition with different zinc contents leads to a failure of the welding electrode due to the limited nugget size. This is mainly caused by a softening of the electrode cap material. Dupuy (1999) observed that the type of zinc coating on the steel (i.e., galvanized, galvannealed or electrogalvanized material) is of considerable importance. Zinc, which is in the coating of hot-dip galvanized steel sheets, only rarely reacts with the steel substrate. This leads to an increased amount of free zinc available during the welding process. On the other hand, galvannealed surfaces that consist of a zinc–iron alloy do not contain any free zinc. The welding electrode therefore reacts differently to

* Corresponding author.
E-mail address: michael.spitz@voestalpine.com (M. Spitz).

http://dx.doi.org/10.1016/j.jmatprotec.2014.09.011
0924-0136/

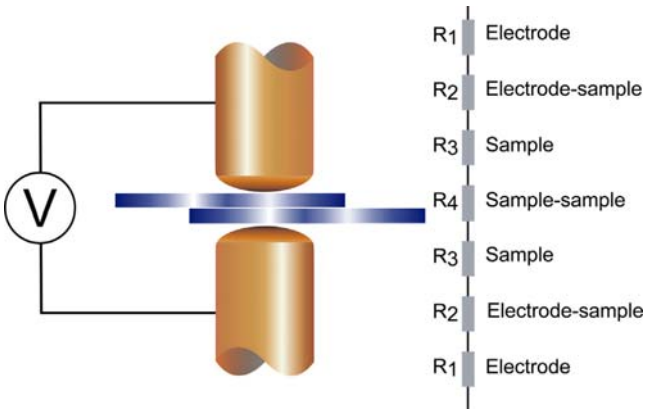

Fig. 1. Schematic illustration of resistances. Voltage drop is recorded from electrode to electrode.

these two types of chemical compositions (zinc or zinc–iron alloy) in the coating surface during resistance welding.

The objective of this work was a detailed characterization of the material-uptake phenomena exhibited by welding electrodes for two predefined surface states of hot-dip galvanized steel sheets: lubricated and non-lubricated. Previous electrode-life tests have shown that welding characteristics differ according to the type of lubricant used. Proper selection of the lubricant is of significant importance to optimized weldability, for example, with respect to the resistance spot welding of hot-dip galvanized steel sheet with a zinc or zinc–aluminum–magnesium coating. Detailed knowledge of the mechanisms of how lubrications affect the resistance spot welding of hot-dip galvanized steel sheets is fundamental to process optimization.

Analytical characterization of welding electrode imprints as well as welding electrode surface caps for an increasing energy input was done using, for example, energy dispersive X-ray spectroscopy element mapping. This procedure demonstrated the main differences that arose between lubricated and non-lubricated hot-dip galvanized steel sheet surfaces. Dynamic conduction resistance curves could be correlated to the electrode cap material uptake during the resistance spot welding process. Analysis of the evolving welding fume revealed the major difference between the two selected surface states during resistance spot welding. Lubrication permits material removal from the electrode-sample interface during the welding process. Fewer and differently distributed deposits remain on the electrode cap surface, in particular zinc. Furthermore, reduced sticking of welding electrodes could be attributed to the influence of lubrication.

A model for electrode material uptake is presented, which schematically illustrates the different deposition mechanisms of material from the welded surface onto the welding electrode for lubricated and non-lubricated hot-dip galvanized steel sheet surfaces.

2. Experimental

Resistance spot welding experiments were performed on a standard 50 Hz pedestal-type welding set-up. Dynamic conduction resistance and energy values were calculated from the recorded welding current and voltage. Voltage drop was determined across the total stack of resistances from electrode to electrode (Fig. 1), and the welding current was evaluated using a Rogowski coil.

Rogowski and Steinhaus (1912) first presented major current data recording results by means of the voltage that is induced in an electrical conductor perpendicularly oriented to the current path. This voltage is based on the magnetic field accompanying the welding current. A material-dependent welding force and the welding time were selected according to standard technical regulations. Welding electrodes (i.e., type D, d_1 = 16 mm, d_2 = 5.5 mm, $\alpha = 31^\circ$, domed) were dip-dressed prior to each experiment, which provided a defined reproducibility of starting conditions. The surface state of the welding electrode was checked electrically. This was done by recording the conduction resistance of bare welding electrodes without a steel sheet sample for a welding current of 3.0 kA. A change in the electrode cap surface by the penetrating current could be neglected according to the low current and low contact resistance of the electrode-electrode interface. With this approach, changes in the surface condition could be monitored prior to the experiment such as an oxidation of electrode caps or a change in dip-dressing procedure.

Experiments were performed on the same base material, i.e., hot-dip galvanized mild steel (voestalpine, DX54D, steel sheet thickness = 0.98 mm zinc layer thickness = Z100 corresponding to 7 μm on each coated face) to prevent an influence caused by the steel substrate. This influence is well known for resistance spot welding due to the strong dependence of welding parameters on steel grade and thickness. Additional cleaning of the sample surfaces ensured comparable starting conditions for each experiment. This comprised an alkaline rinsing bath and, if welded in the lubricated state, precisely defined re-lubrication conditions. Chemical cleaning was controlled by contact time and rinsing concentration to ensure an unchanged Al_2O_3 layer on top of the hot-dip galvanized coating. Maaß and Peißker (2008) directly correlated this native layer on hot-dip galvanized coatings to the aluminum content in the zinc bath, i.e., 0.2 wt% in this case. Surface lubrication was applied on the steel sheet surface by means of a laboratory coating, i.e., Multidraw® PL61 a deep-drawing lubricant. The thickness of this layer was defined at 1 g/m^2 although the amount of lubrication on the surface was not relevant for the final welding results. In order to limit surface oxidation, welding experiments were performed within 30 min after the cleaning process.

Conducted experiments were subdivided into energy-dependent, standard-welding and welding-fume experiments.

1 Energy dependent experiment:

The aim was the detailed determination of material uptake of the welding electrode from the sample surface during resistance spot welding. The time/energy-dependent evolution of the electrode-substrate interaction was analyzed in two ways: In one set of experiments, a series of spots was welded on a pair of galvanized steel sheets with a stepwise increase of the welding current (2.0 kA up to 8.9 kA) for a defined number of welding times (11 periods, until a predefined energy input for the last spot was reached as measured by the size of the welding nugget). In the other set of experiments, the welding current was fixed and the number of current periods was increased for each welded spot (from a single half wave to 11 periods) until the predefined energy input was reached as outlined above. For each series, one steel sheet sample was welded for each set of parameters (i.e., 40 mm × 60 mm). Naturally, each imprint on the sample surface could be analyzed for each energy input, whereas the electrode cap surfaces were analyzed after the last spot of a series.[1] The energy entry was calculated from Eq. (1).

$$\Delta Q = R \cdot I^2 \cdot \Delta t \quad (1)$$

R denotes the calculated dynamic conduction resistance; I the measured current; t the welding time; and Q the energy input, respectively. Current and voltage values were integrated from

[1] No significant change in welding electrode cap material uptake during energy-entry increase could be observed from prior conducted experiments

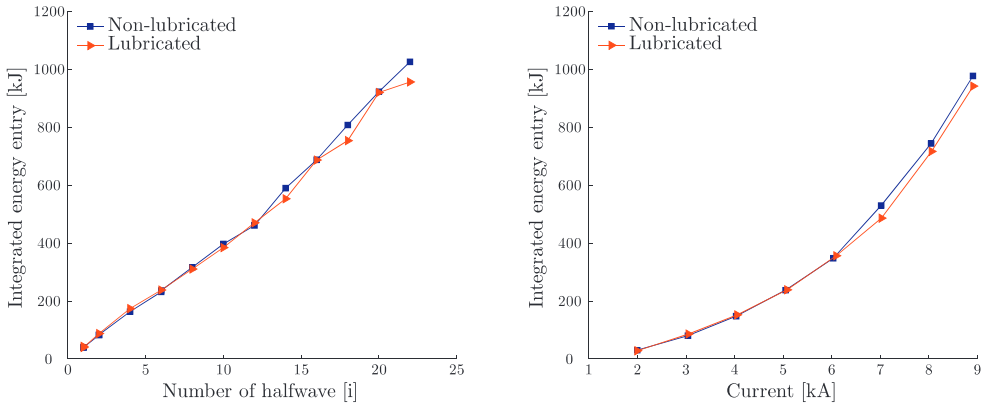

Fig. 2. Application of a time-dependent energy input (left) results in a higher total energy value for the last welded spot. Firstly, this can be attributed to the integrated energy input that corresponds to the higher curves in the linear case. Secondly, welding electrode material uptake varies due to an unequal number of contacts with the sample surface up until the end of the experiment. However, contact formation and electrode cap coverage is comparable for the different increasing energy curves.

the recorded raw data by means of true root mean square calculation (phase-fired control). Electrode imprints on the sample surface for each energy input and the electrode cap surface after the last energy input were characterized applying light microscopy as well as by energy dispersive X-ray spectroscopy element mapping.[2] The latter provides information on the distribution of material deposition on the welding electrode cap. Polished cross section samples (center of electrode caps as well as imprints) were analyzed by a scanning electron microscope. On the one hand, this was done to determine the interaction of deposit elements with the electrode base material, e.g., alloy formation, and on the other hand, to estimate the thickness of the deposition on the welding electrode cap.

2 Standard welding experiment:

100 and 900 spots were welded on one sample (i.e., 300 mm x 300 mm), to evaluate deposits on the electrode cap for standard welding conditions. The applied welding current is selected in the middle of the welding range at 8.9 kA. Characteristic values were the integrated dynamic conduction resistance and the integrated energy input per welded spot throughout the duration of the experiment. Welding electrode caps were analyzed after the complete welding process using energy dispersive X-ray spectroscopy element-mapping on the surface and on the polished cross sections.

3 Welding fume experiments:

Differences in element concentrations exhausted from the electrode sample as well as the sample-sample interfaces during welding were quantified for the lubricated and non-lubricated surface states. Firstly, the weight of coarse particles remaining in the absorbing glass chamber and the weight increase of the absorbing filter were determined compared to the weight prior to the welding experiment. Secondly, metallic elements filtered from the welding fume were analyzed chemically.[3]

3. Results and discussion

3.1. Energy dependent experiment

Electrode-sample interaction by means of an integrated energy input for each welded spot up until the last spot is different for the increasing energy curves in general (time-linear and current-quadratic: Fig. 2). For an identical current, an identical energy input was expected. However, the energy input after the last spot differed for the different energy input variations. It was higher in the linear case. Furthermore, the electrode cap deposit also varied. It was more pronounced for the time-dependent energy input as can be seen in the electrode image in Fig. 3. Both observations could be correlated to the higher integrated energy input and a disproportionate higher number of contact spots during the time-dependent experiment conducted in a step-wise manner.

Contact formation and its evolution during an increasing energy input was different for the lubricated and non-lubricated surfaces. This difference did not depend on the energy input increase, i.e., time- or current-dependent. Grooves remaining on the electrode cap after dip dressing were only visible within the electrode imprints on the cleaned surface for low energy inputs, i.e., 2.0 kA and 0.5 periods, respectively. Scratches were located along the edge of the contact area, i.e., at the position of the highest pressure during resistance spot welding, especially with domed electrodes.[4] Contrary to this, lubrication provided a mechanical barrier between the contact surfaces. Additionally, lubrication led to a reduced melting of the sample surface for an increasing energy input. A bright appearing homogeneous electrode imprint remained on the non-lubricated sample surface for the highest energy input. The counterpart exhibited a dark gray circle in the center of the imprint surrounded by an outer ring with a brighter appearance.

Lubrication led to the formation of a silvery concentric circle on the electrode cap surface as opposed to a homogeneous layer formation for the non-lubricated steel sheet surface. Both observations correlated with the corresponding electrode imprints on the sample surface.

The zinc content was apparently lower within the remaining electrode imprint and on the electrode cap surface for the case with surface lubrication. Zinc coverage was homogeneous on the welding electrode and within the electrode imprints for the non-lubricated case. The same is valid for the iron content within the electrode imprints. According to Jordan and Marder (1997) zinc–iron phases are known to form at an early stage of an annealing process of hot-dip galvanized steel sheets. Additionally, the aluminum content was higher for the welding electrode cap in the non-lubricated case. A reduced zinc and iron content within the electrode imprint and a reduced zinc and aluminum content on the electrode cap surface led to the following preliminary explanations:

[2] Energy dispersive X-ray spectroscopy element mapping was performed to highlight the local distribution of elements on welded electrode cap surfaces.

[3] Welding fume experiments were performed according to SEP 1160. Analysis and welding procedures are defined in this regulation.

[4] Rashid et al. (2009) demonstrated by simulations and experiments that this effect results with domed electrodes. Material deformation with increasing pressure leads to a concentration of the load at the edge of the contact area.

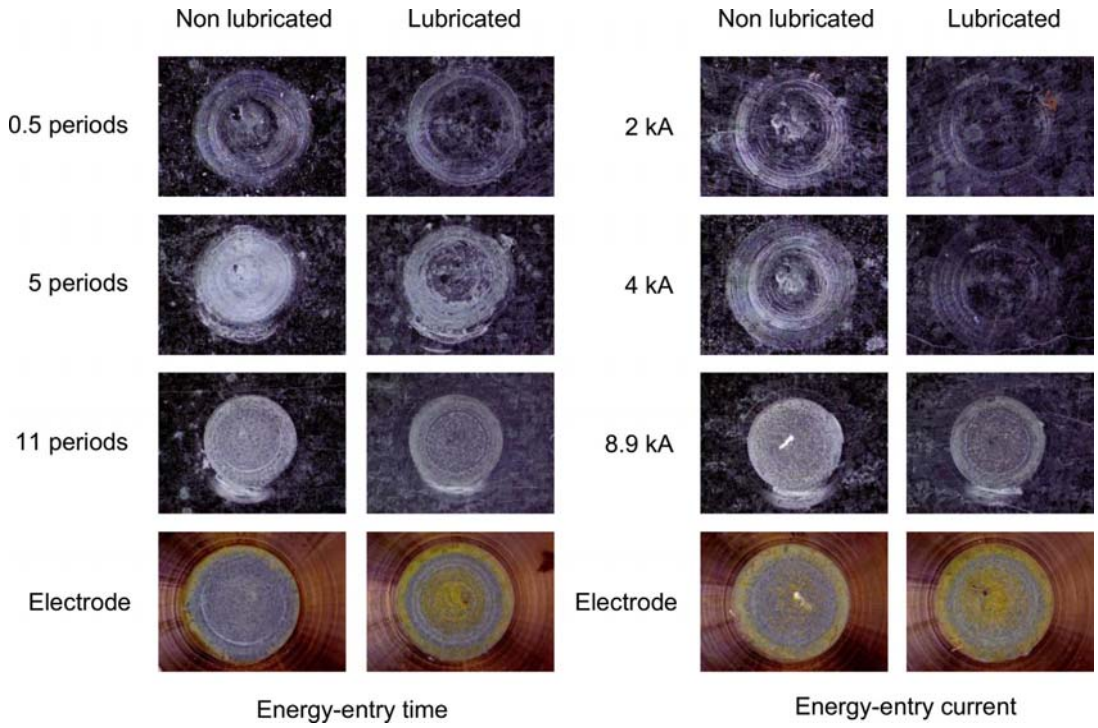

Fig. 3. Electrode imprints on the lubricated and non-lubricated sample surfaces and electrode cap surfaces for the different energy-input variations. Surface lubrication hindered the mechanical and electrical interaction of the electrode sample. Layer formation on the welding electrode cap surface varied according to the surface conditions.

- A lower temperature at the contact interface retarded the zinc–iron alloy formation for the case when lubrication was applied
- A lower zinc/aluminum content within the interface or a diffusion barrier due to surface lubrication led to a reduced alloy formation

Energy dispersive X-ray spectroscopy supports element-mappings of electrode imprints and of electrode cap surfaces respectively. Based on the identical layer formation of both energy-increase variants, the results of element mappings are presented in the time-dependent variant only (Fig. 4). Naturally, carbon could be observed on both surfaces: both on the welded electrode and within the electrode imprints (Table 1). Carbon detected for the case with non-lubricated surfaces could be related to the composition of the carbon steels as well as to surface carbonation from ambient air. Therefore, a quantitative analysis of the carbon content is not in the scope of this work.

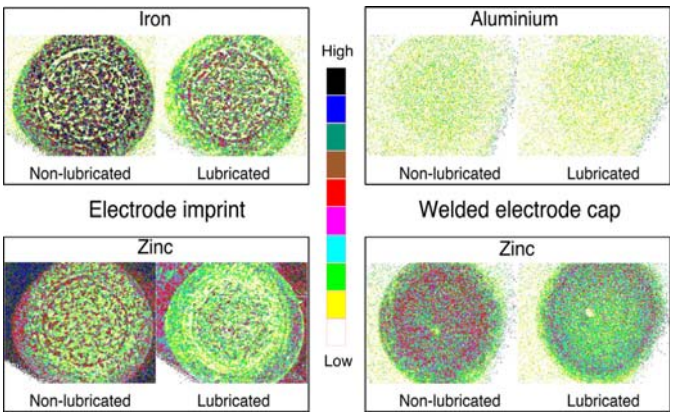

Fig. 4. Energy dispersive X-ray spectroscopy mapping of electrode imprints (acceleration voltage: 20 kV) and the corresponding welding electrode cap surfaces with the highest energy input for the time-controlled energy variant. Zinc distribution is clearly different for both surfaces, additional aluminum is visible for the electrode cap, and increased iron in the electrode imprint. Lower zinc and iron contents within the electrode imprints could be observed for the case with surface lubrication. Lubrication formed a barrier layer that limited a chemical interaction with the contact surfaces.

Table 1
Quantified element mapping of welding electrode imprints and electrode cap surfaces. Significant differences in the zinc, iron and carbon contents could be observed for the electrode imprints, e.g., electrode imprint and the electrode cap welded on the lubricated surface exhibited a smaller zinc content. The carbon content only indicated surface lubrication in this case. Only elements are depicted, that clearly indicate differences past spot welding. The sum of all contents is not 100 %, thus.

	Non-lubricated (wt%)	Lubricated (wt%)
Electrode imprint		
Zn	39	22
Fe	25	13
Cu	5	2
C	28	61
Electrode cap surface		
Zn	37	22
Fe	0.7	0
Al	0.8	0.5
C	30	46

Energy dispersive X-ray spectroscopy element mappings were quantified to correlate with the respective visual differences (Table 1).[5] The zinc content within the electrode imprint and on the electrode cap surface was approximately doubled in the non-lubricated case. This was also true for the iron content within the

[5] Quantification of energy dispersive X-ray mappings on different sample surfaces was rarely reproducible within a sufficiently small range – error margins were strongly dependent on the position of the sample undergoing analysis. The cited values are therefore used as a general indication only. Not all quantified elements are presented in the tables, only elements that showed relevant differences. The sum of all quantities is not 100%, thus.

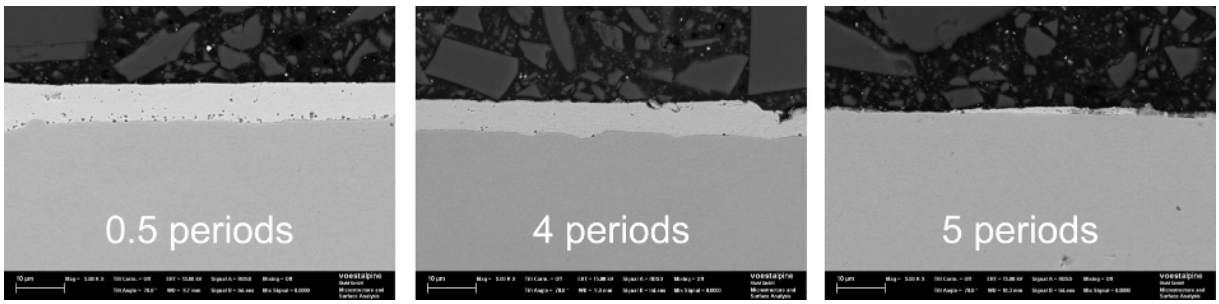

Fig. 5. Cross section through the center of selected electrode imprints on the lubricated sample (0.5, 4 and 5 periods of energy increase with time). The native zinc layer was compressed with an increasing energy input (left and centered picture). After four welded periods, i.e., a threshold energy input for the selected welding parameters, zinc was only locally found on the surface. The energy threshold was identical for the non-lubricated sample. Despite a zinc loss in all samples, aluminum could be detected at the location of the native barrier layer, i.e., between the zinc layer and the steel sheet.

electrode imprint. The carbon content was, of course, inverted due to surface lubrication. A higher copper content within the electrode imprint on the non-lubricated surface evidenced a higher contact temperature of the electrode sample, i.e., copper diffusion was more likely from the welding electrode towards and into the sample surface at elevated temperatures. The same statement is valid for the higher iron content which was detected on the corresponding welding electrode cap surface. Additionally, the oily barrier limited chemical interaction in general in the lubricated case.

Aluminum could almost not be detected on the electrode cap for the case with surface lubrication. The total aluminum content on the electrode cap surface in the non-lubricated state was extremely high compared with the low aluminum content in a hot-dip galvanizing bath: 0.8–0.2 wt% in the bath (Table 1). In order to understand the origin of this unexpected high aluminum content on the electrode cap surface, welded joints of the different energy inputs were analyzed (Fig. 5).

Metallographic cross sections were made in the center of the imprints of the joined metal pieces of welding electrodes after welding. Scanning electron microscope images depict the outermost layer on the upper side of the welded stack. A continuous zinc layer was visible within the electrode imprint up until a certain energy threshold, in this case, after four welded periods for both surface conditions. The thickness of the native zinc layer was only compressed with time as a result of the applied load of the welding electrodes and the temperature increase. Above this energy threshold almost no zinc could be found on the steel sheet surface, i.e., only a thin non-continuous layer of zinc remained. Zinc was either squeezed out of the interface or evaporated, or both. For all energy inputs, local energy dispersive X-ray spectroscopy revealed an aluminum content still present on top of the steel sheet surface, i.e., at the position of the former native barrier layer. This was also valid for regions where no zinc remained on the surface. According to Kato et al. (2000), zinc–iron phases form from the iron–aluminum–zinc barrier layer without aluminum depletion at the beginning of an annealing process where there is an increase in the energy or current. With increasing energy levels, there will be an intermixing within the zinc layer (The reader should note that the cited literature deals with incomparably long process duration times, i.e., those characterized by seconds as opposed to milliseconds in the case of joint formation applying resistance spot welding. However, the energy input per time unit is much higher in the welding process.). Contrary to this, aluminum remained on the steel sheet surface. A native barrier layer contains a comparatively high amount of aluminum (60 wt%) of the total content in the hot-dip galvanized zinc layer. Thus, with increasing energy the welding electrode interacted with this “higher” aluminum content on the steel sheet surface and, as a result, a portion of this amount was deposited on the electrode cap surface. Compared to the zinc bath concentration, a higher aluminum content on the welding electrode was therefore not surprising. Nevertheless, surface lubrication limited the uptake of aluminum.

3.2. Standard welding experiment

This section was subdivided into an early stage of electrode degradation with 100 spots and a more advanced stage with 900 spots. The first part describes the evaluation of electrode material uptake (mainly zinc in this case) via dynamic conduction resistance. The second part highlights the final deposition on the electrode cap.

3.2.1. 100 spots

Different material uptakes for lubricated and non-lubricated surface states also occurred for the increase of number of welded spots, as depicted in Fig. 6.

A non-lubricated surface resulted in a uniform, radially symmetrically centered silvery deposition on the welding electrode cap surface. As opposed to this, a dark appearing area surrounded by a silvery ring developed on the electrode cap surface for the case with lubrication. Here, no radial symmetry could be observed. Selected imprints from a series of welded spots (1, 50 and 100) revealed similar distinctions. All imprint areas on the non-lubricated surface appeared brighter than on a lubricated surface. This could again be correlated with a higher zinc content in the electrode-surface interface (Table 1). For both cases, visual impressions of electrode

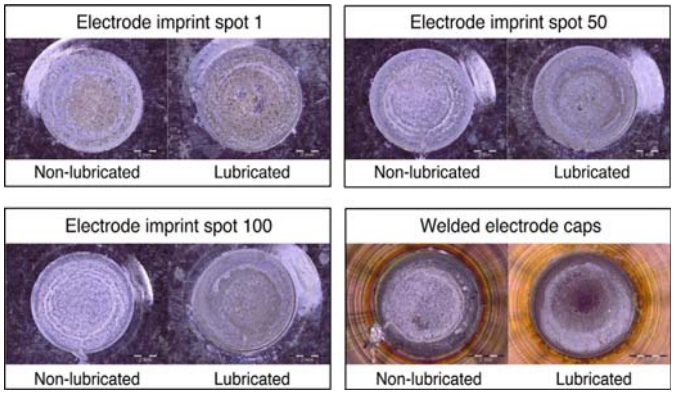

Fig. 6. Selected electrode imprints after 50 and 100 spots, and welded electrode caps after the final spot. Material deposition on the electrode cap surfaces and within the electrode imprints differed optically, i.e., brighter appearing areas were visible for the non-lubricated surface, which indicated a higher zinc content. The zinc content was reduced on each surface due to lubrication. Zinc therefore must have been transported outwards from the contact interface, either mechanically (by additional squeezing) or physically (by evaporation).

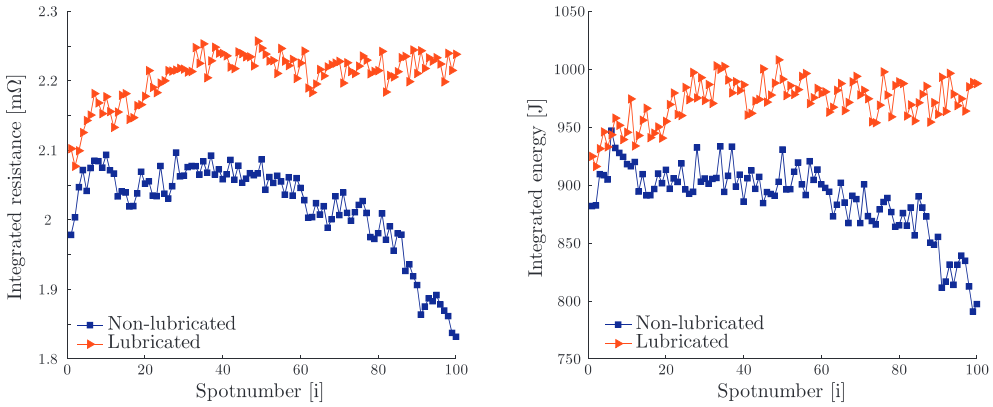

Fig. 7. Evolution of integrated conduction resistance and energy during spot welding of 100 spots. A significant decrease for the non-lubricated surface corresponded to different layer formations on the welding electrode cap surface. This was the result of a lower contact resistance associated with the higher zinc content. Surface lubrication provides process stability.

imprints correlated with the electrode cap surface deposition distribution, e.g., radial symmetry for the non-lubricated surface.

Different welding characteristics could be additionally observed by means of dynamic conduction resistance (Eq. (2)) and energy input (Eq. (3)) – both values integrated over time, i.e., the area under the particular curve.

$$\text{Integrated conduction resistance} = \int_{t_1}^{t_2} R \;\; dt \tag{2}$$

$$\text{Integrated energy} = \int_{t_1}^{t_2} (R \cdot I^2) \;\; dt \tag{3}$$

Here, t_1 and t_2 denote the start- and stop-time for welding a single spot, respectively.

Gedeon et al. (1987) introduced the evaluation of the dynamic conduction resistance during resistance welding, i.e., resistance dependence on welding time. The specific shape of this curve permits the differentiation among different coating systems, e.g., a bare steel surface and a zinc-coated steel sheet, respectively. Here, a different presentation of these data was selected, i.e., integrated values.

At the beginning of the experiment, resistance and the energy increase were similar for both surface variants, i.e., spots one to ten (Fig. 7). This increase is associated with the alloying of the electrode cap material with components of the sample (mainly zinc) at the beginning of a resistance spot welding process. Starting from the tenth welded spot, the shape of the different curves evolved divergently. For the lubricated system, energy and resistance curves increased until reaching a saturation level, unlike the non-lubricated system values that decreased from spot 40 until spot 100. The reason for this opposite behavior was correlated to the varying material deposition on the welding electrode cap, i.e., more zinc was taken up by the welding electrode from a non-lubricated surface during the welding process. On the one hand, the latter led to an improvement of the contact situation during the welding process that was caused by an increase of the contact area and the benefit of a zinc–zinc electric contact, which decreased the contact resistance at the beginning of the welding process. On the other hand, a higher zinc content on the welding electrode cap surface leads to the final failure of the welding electrode in general (see Parker et al., 1998). Surface lubrication led to a smaller variation of the energy input and dynamic conduction resistance. This resulted in more constant nugget diameter with time and thus improved weldability.

3.2.2. 900 spots

Increasing the number of resistance-spot-welded joints to 900 spots revealed no further changes in the material uptake of the welding electrode. Lubrication again led to a decentralized formation of material deposition on the electrode cap surface compared to a radial symmetric deposition in the non-lubricated case. Energy dispersive X-ray spectroscopy element mappings confirmed the visual impression. The same elements with a different local distribution were observed for the two surface conditions (Fig. 8).

- Non-lubricated surface

  Concentric deposition on the welding electrode cap was mainly built from aluminum and oxygen, most probably as Al_2O_3 This layer led to a low electrical conduction in the center of the conducting interface. Current flow was therefore restricted to the edge of the contacting area and to local conducting paths within the high-resistance region. Current constriction led to an increased local energy input with a high current density and a high local temperature. Thus, material and element diffusion was promoted because of the higher temperature in the contact area, i.e., iron from the base material migrated towards the welding electrode and copper from the electrode towards the steel sheet surface. A more electrically conductive zinc ring surrounded the central depositions. Iron was also present in the center area (locally accumulated, as explained above), but the main amount

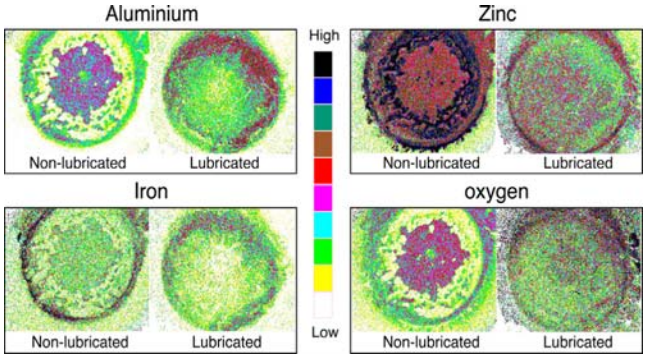

Fig. 8. Differences in electrode material uptake could be highlighted by energy dispersive X-ray element mapping (acceleration voltage 20 kV). Elements building low/non-conducting compounds were found in the center of the welding electrode cap surface in the non-lubricated case. Depositions were concentrated north east aside the center of the welding electrode cap in case of surface lubrication, i.e., the current path was less hindered according to the specific deposition distribution in this case.

Table 2
Resistance spot welding for lubricated and non-lubricated hot-dip galvanized steel sheets led to different weights of coarse particles that accumulated in the collecting glass unit and also as fine dust in the filter. In the case for lubricated surfaces, an increase in the exhausted particles could be already visually observed in the form of a smoky vapor within the glass construction.

Particle weight	Coarse particles (mg/spot)	Fine dust (μg/spot)
Non-lubricated	$4.5 \pm 0.9 \times 10^{-02}$	1.9 ± 0.9
Lubricated	$13 \pm 3.6 \times 10^{-02}$	33 ± 5.2

was concentrated near the edge of the contact region of the electrode cap surface.

- Lubricated surface

  Material depositions on the electrode cap surface were distributed along the outside of the electrode cap face, with the exception of carbon. A sickle-like deposition could be found northeast of the center that formed from aluminum, iron and oxygen. On the opposite side, and in the remaining area in the center, a small amount of zinc was observed. The main portion was concentrated on the edge of the contact area. Therefore, current flow in the center of the spot was not (or at least less) hindered.

3.3. Welding fume experiments

The zinc content was lower on the electrode cap and within the electrode imprints in the case with surface lubrication. An explanation for this observation could be evaporation and/or mechanical removal from the conducting interface. Lubrication was presumed to promote both mechanisms. Welding fume developing during the welding process between the conducting interfaces that was finally exhausted into the ambient air was analyzed to clarify zinc loss in detail. Fig. 9 depicts the glass construction cell that was evacuated by a roughing pump during the experiment. As a first step, the weight of coarse particles – i.e., particles that deposited within the glass construction prior to a dust filter – was analyzed. The particles were brushed out of the glass chamber using a paint brush. In a second step, fine dust and metallic components were removed from the filtered welding fume. The weight of the filters was recorded before and after the welding procedure. Furthermore, a reference filter was ventilated through the glass construction in order to evaluate possible influence from the surrounding area. The results were corrected for this background value.

Lubrication led to a higher quantity of coarse particles and fine dust compared to the non-lubricated surface (Table 2). The weight increase was different for coarse particles and fine dust, i.e., by a factor of 3 and 15, respectively. A reasonable explanation for this difference was the fact that particles collected by the filter were not subdivided into metallic and organic substances – for example, oil drops deposited within or on the registering filter. Therefore, a portion of the additional fine dust weight that was registered in the case of surface lubrication could be attributed to oil fumes. However, the weight increase was noticed.

Metallic particles in the welding fume were chemically removed from the filter after welding (Table 3). A 60-times-higher quantity of zinc was detected for the lubricated surface compared to the non-lubricated one. Elements that were assumed to affect a resistance-welding process in a negative way, i.e., mainly zinc, were efficiently removed from the electrode-sample interface in the presence of lubrication. Additionally, a lower iron content in the welding fume suggests a lower contact temperature during the welding process. This might be related to a cooling effect from the exhausting process at the contact interface. Moreover, material transport formed an additional barrier layer that limited sticking of the welding electrode cap. These results indicate an efficient material-removal mechanism for lubricated surfaces, which explains the above-mentioned lower quantity of adverse elements such as zinc in the contact area.

Table 3
Metallic elements in the welding fume collected by the filter. Lubrication led to a zinc increase in the welding fume by a factor of 60. A lower iron content correlates to an additional cooling of the electrode-sample interface during the welding process. A lower zinc quantity in the interface limits electrode degradation in general.

Filtered metallic elements	Iron (μg/spot)	Zinc (μg/spot)
Non-lubricated	3.1	0.2
Lubricated	2.5	13.4

3.4. Examples of welding electrode material uptake

Fig. 10 depicts a schematic model that combines the obtained results. The time evolution of the welding process is presented in a sequence of steps that start from the mechanical contact formation up until the moment when exhausting occurs in the case of surface lubrication (approximately period four). It is to be noted that the last stage is not the end of the welding time – a welding nugget will form after this stage.

1 Electrode approach

  The first difference was observed for the primary mechanical contact of the electrode cap and sample surface. Lubrication led to a minimized mechanical contact and therefore resulted in a changed electrical contact such as a restriction of the current path to the edge of the conducting area.

2 Electrode force increase

  Whereas the non-lubricated surface formed a mainly metallic contact with the welding electrode, lubrication led to the formation of a barrier layer. This was even true in the case of an increased load. (It was not possible to completely squeeze oil out of the interface). This oily barrier layer led to a sole partial mechanical contact that was located mainly at the position of maximum load. In the case that lubrication was absent, a primarily mechanical seal formed proportional to the applied pressure. It is to be noted that this difference was present without a welding current.

3 Current/energy increase

  A welding electrode would directly interact with the native zinc layer in the case with a non-lubricated surface. This was in contrast to the hindered electrical contact through the lubrication layer that separated the surfaces. A native iron–aluminum–zinc barrier layer between the zinc-layer and steel sheet would be transformed during this energy increase, resulting in the formation of zinc–iron phases. This transformation led to an increased aluminum content on the steel sheet surface even if zinc was already absent.

4 Material transport

  For both surface conditions a different zinc content was observed after a certain energy threshold on the electrode cap surface as well as within the electrode imprints, for example, after period four for the selected set of parameters. A reduced zinc quantity was noted in the case of a lubrication-promoted material transport away from the electrode-sample interface. Lubrication offered the possibility to develop a path of material transport through the mechanical barrier at the edge of the contact area. In the non-lubricated case, the mainly pressure-induced mechanical ring-shaped metallic seal trapped material to a higher degree in the contact interface. Absence of the lubrication barrier layer increased the possibility for chemical interaction of the welding electrode cap and the sample surface components. For example, the formation of alloys additionally increased the strength of the

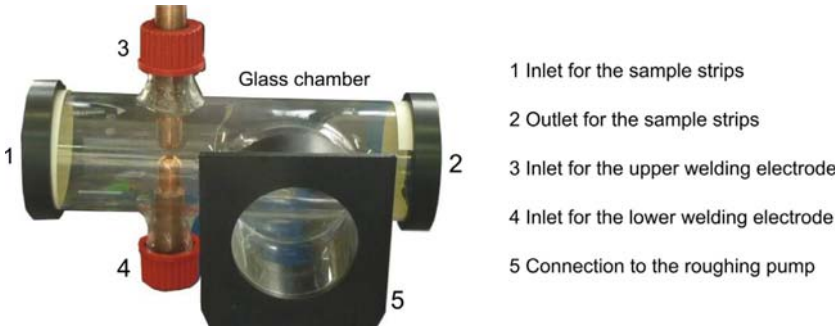

Fig. 9. Glass construction for collecting welding fume that was exhausted during resistance spot welding. Steel sheet samples were inserted into the housing through slits within the black lids to close the housing as seen in the left and right side of the picture (1,2). Exhausted welding fume was extracted through a filter by means of a roughing pump. The filter was positioned before the roughing pump and after the housing opening at the front of the picture (5).

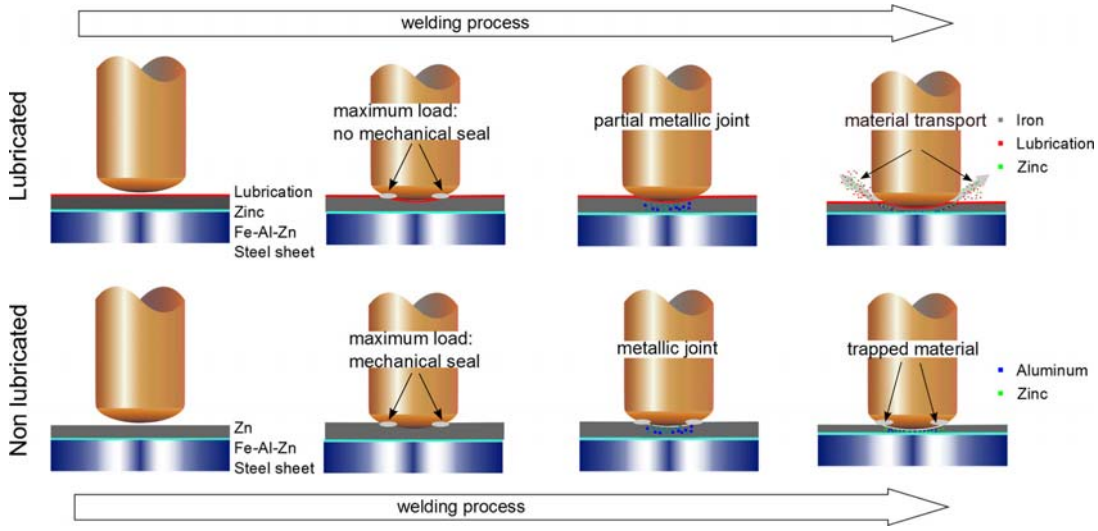

Fig. 10. Examples of possible processes that could result in different weldability characteristics for lubricated and non-lubricated hot-dip galvanized steel sheets. The time-line is depicted from the left to the right. The main difference can be related to the oily barrier layer that leads firstly to a different electrical contact, secondly to a different evolution of the mechanical contact and finally to a different material transport away from the contact interface.

mechanical seal. Sticking of welding electrodes could be directly correlated to this alloying.

4. Conclusions

Superior weldability of lubricated hot-dip galvanized steel sheet surfaces could be directly related to the following results:

- Absence of surface lubrication led to the formation of a non-/low electrical contact layer (e.g. Al_2O_3) on the welding electrode cap surface. Current path was restricted to narrow paths, energy entry was increased and element diffusion was increased in the contact interface. Electrode life decreased.
- Surface lubrication minimized the interaction of zinc and aluminum with the welding electrode cap. Far more zinc is exhausted to the surroundings during the welding process in this case. As a result, the formation of brass alloy layers on the welding electrode cap was hindered. Electrode life could thus be increased.
- Surface lubrication reduced the local energy input as a result of the cooling of the electrode surface. Reduced alloying within the contact interface and additional heat removal from the interface during the welding process could be observed.
- Sticking of the welding electrode cap was hindered in the presence of lubrication. A barrier layer had already formed initially between the welding electrode and the sample surface without the welding current. This reduced electrode wear in accordance with the deep-drawing characteristics of the lubrication. Secondly, limited interaction between the welding electrode and the brass-alloy formation subsequently reduced sticking, even with an increased welding current.
- A schematic model of the beneficial effects of surface lubrication for a resistance spot welding process could be demonstrated.

Acknowledgments

This work was supported by voestalpine, Henkel and CEST and funded within the COMET program by the Austrian Research Promotion Agency (FFG) and the government of Lower Austria. Inspiring discussion with F. Perndorfer is acknowledged.

References

Dupuy, T., 1999. The degradation of electrodes by spot welding zinc coated steels. Weld. World Lond. 43 (6), 58–68.
Gedeon, S., Sorensen, C., Ulrich, K., Eagar, T., 1987. Measurement of dynamic electrical and mechanical properties of resistance spot welds. WRC Bull. 322, 378–385.
Han, L., Thornton, M., Boomer, D., Shergold, M., 2010. Effect of aluminium sheet surface conditions on feasibility and quality of resistance spot welding. J. Mater. Process. Technol. 210 (8), 1076–1082.
Jordan, C., Marder, A., 1997. Fe–Zn phase formation in interstitial-free steels hot-dip galvanized at 450° c: Part II 0.20 wt. J. Mater. Sci. 32 (21), 5603–5610.

Kato, T., Nunome, K., Kaneko, K., Saka, H., 2000. Formation of the gamma phase at an interface between an Fe substrate and a molten 0.2 mass. Acta Mater. 48 (9), 2257–2262.

Maaß, P., Peißker, P. (Eds.), 2008. Handbuch Feuerverzinken. John Wiley & Sons, March 2012.

Parker, J., Williams, N., Holliday, R., 1998. Mechanisms of electrode degradation when spot welding coated steels. Sci. Technol. Weld. Join. 3 (2), 65–74.

Rashid, M., Fukumoto, S., Medley, J., Villafuerte, J., Zhou, Y., 2007. Influence of lubricants on electrode life in resistance spot welding of aluminum alloys. Weld. J. N. Y. 86 (3), 62.

Rashid, M., Medley, J., Zhou, Y., 2009. Electrode worksheet interface behaviour during resistance spot welding of al alloy 5182. Sci. Technol. Weld. Join. 14 (4), 595.

Rogowski, W., Steinhaus, W., 1912. Die messung der magnetischen spannung. Arch. Elektrotech. 1 (4), 141–150.